Forensic Science International 365 (2024) 112278

Contents lists available at ScienceDirect

Forensic Science International

journal homepage: www.elsevier.com/locate/forsciint

A first step towards a machine learning-based framework for bloodstain classification in forensic science

Hyeonah Jung [a,1], Yeon-Soo Jo [b,1], Yoseop (Joseph) Ahn [a], Jaehoon (Paul) Jeong [a,*], Si-Keun Lim [b,**]

[a] Department of Computer Science and Engineering, Sungkyunkwan University, Suwon, Gyeonggi-Do 16419, Republic of Korea
[b] Department of Forensic Sciences, Sungkyunkwan University, Suwon, Gyeonggi-Do 16419, Republic of Korea

ARTICLE INFO

Keywords:
Forensic science
Machine learning
Bloodstain
Pattern
Classification

ABSTRACT

Bloodstains found at a crime scene can help estimate the events that occurred during the crime. Reconstructing the crime scene by analyzing the bloodstain pattern contributes to understanding the bloody event. Therefore, it is essential to classify bloodstains through bloodstain pattern analysis (BPA) and accurately estimate the actions that took place at that time. In this study, we investigate the potential of using machine learning and deep learning to determine an action related to bloodstain data through the accessment of the corresponding bloodstain type by creating a prototype classification model. There are 14 types of bloodstain according to the classification system based on appearance. In this study, we test the classification potential of each bloodstain data for three bloodstain patterns such as Swing, Cessation, and Impact. Through experiments, it is shown that our prototype classification model for the selected bloodstains is developed and the accuracy of the resulting model is evaluated to be 80 %.

1. Introduction

Bloodstain Pattern Analysis (BPA) [1] is a pivotal aspect of forensic sciences, vital for reconstructing events at a crime scene. The relevance of bloodstains in forensic investigations is beyond dispute. Such remnants provide invaluable insights into event sequences, connections between the attacker, victim, and crime scene, and also offer unique DNA-based identifiers [2]. Traditional methods, however, can falter, especially when dealing with overlapping or intricate bloodstain patterns. Additionally, these methods rely significantly on the subjective interpretations of analysts, making them time-consuming [3,4].

Historical examinations of bloodstain classifications reveal a taxonomy rooted in morphology and generation mechanisms. Seminal works by Tom Bevel and Ross M. Gardner have provided foundational blueprints for BPA [5]. These paradigms have assisted in identifying the activities of the victim and attacker from determining their positions and actions, respectively, for the bleeding in the crime. However, as forensic science advances, there is a need to efficiently perform complex tasks (e.g., AI-based analysis rather than human-based analysis for bloodstain pattern recognition) that are difficult to perform with traditional methods.

In our goals to further enhance this BPA, we have integrated the capabilities of Artificial Intelligence (AI) and Machine Learning (ML). Recognizing the growing role of AI and ML in modern forensic sciences and its proven track contribute to optimizing workflows and reducing manual intervention. So we expect three primary outcomes from our approach. Firstly, we anticipate a markable improvement in the reliability of BPA results. Secondly, using AI-driven techniques should considerably lessen the time and resources that investigators dedicate to reconstructions. Lastly, by leveraging AI, we are positioned to extend our research into the identification and analysis of various trace evidences, encompassing fingerprints, tool marks, footprints, and tire tracks.

Leveraging AI's computational strengths, our research is geared towards creating a classification scheme that promises not only a more precise categorization of bloodstains but also brings to light the finer

* Corresponding author at: Department of Computer Science and Engineering, Sungkyunkwan University, Suwon, Gyeonggi-Do 16419, Republic of Korea.
** Corresponding author at: Department of Forensic Sciences, Sungkyunkwan University, Suwon, Gyeonggi-Do 16419, Republic of Korea.
E-mail addresses: hyeonah214@skku.edu (H. Jung), joys98@skku.edu (Y.-S. Jo), ahnjs124@skku.edu (Y. Ahn), pauljeong@skku.edu (J. Jeong), sikeun.lim@skku.edu (S.-K. Lim).
[1] As the co-1st authors, Hyeonah Jung and Yeon-Soo Jo equally contributed to this paper.

https://doi.org/10.1016/j.forsciint.2024.112278
Received 15 February 2024; Received in revised form 12 July 2024; Accepted 28 October 2024
Available online 31 October 2024
0379-0738/© 2024 Elsevier B.V. All rights are reserved, including those for text and data mining, AI training, and similar technologies.

details that the traditional methods might miss. To this end, we have employed three AI models, such as Convolutional Neural Network (CNN) [6], Decision Tree [7], and Random Forest [8]. Our goal is to evaluate and determine which among these models offers superior results in bloodstain classification.

In this paper, we unveil a novel methodology empowered by AI, tailored to diminish the inherent biases in BPA and streamline the analytical process. By merging forensic expertise with advanced computational algorithms, our strategy promises to elevate the accuracy and consistency of BPA results. The center of our research is the distinction of three notoriously challenging bloodstain patterns: Swing, Cessation, and Impact. The data preprocessing is integral to the process needed for effective bloodstain pattern classification. The challenge stems from bloodstain images combining distinct stains with their backgrounds.

In particular, the major contributions of this work can be enumerated as:

1. A preprocessing of bloodstain dataset. The background of the photo of bloodstain is removed using the Otsu method technique [9]. By effectively eliminating the background, we are able to better highlight the characteristics of the bloodstains. (see Section 4)
2. A feature analysis for bloodstains with five different characteristics related to bloodstains. For individual bloodstains, the bloodstain's angle, shape, major and minor axis lengths are used, and also for the overall bloodstain distribution, a polynomial equation is used to compute the convex area of bloodstains and the assessment of the comprehensive distribution of bloodstains. (see Section 5)
3. An ML-based classification framework with three ML models. Our framework can adjust the hyperparameters for the three ML models (i.e., the CNN, Decision Tree, and Random Forest) to improve the accuracy of bloodstain classification. (see Section 6)

This paper provides an in-depth exploration of bloodstain classification, detailing the nuanced differences among bloodstain patterns and explaining the origin and significance of each. After building upon this foundational knowledge, this paper presents our AI-driven approach, highlighting its potential to perform forensic bloodstain analysis and its broader implications within forensic sciences. In addition, Fig. 1 shows the overall process of the Bloodstain Type Classification.

The remaining parts of this paper are organized as follows. Section 2 summarizes the related work for bloodstain pattern classification. Section 3 explains the collection method of bloodstain image data. Section 4 explains bloodstain pattern data. Section 5 emphasizes blood feature analysis. Section 6 describes the design and implementation of three ML models. Section 7 evaluates the performance of the ML models in the bloodstain pattern classification. Section 8 concludes this paper along with future work.

2. Related work

Bloodstain pattern analysis (called BPA) is a specialized area within forensic science that examines the physical characteristics of bloodstains found at crime scenes. This includes examining their shape, size, and how they are spread out. By analyzing these traits, experts can infer the events that led to the crime. This method is crucial for criminal investigations as it aids in piecing together the crime scenes and assessing the accuracy of testimonies given by those.

2.1. Bloodstain pattern classification

Bloodstain Pattern Analysis (BPA) examines various characteristics of bloodstains, including their size, location, and shape, to identify the patterns and their underlying causes at crime scenes. Serving as a pivotal segment of forensic science, BPA plays an instrumental role in reconstructing crime scenes and deducing the series of events that happened in the crime. Owing to the fact that bloodstains conform to the laws of physics, their trajectories can be replicated. A stain's direction can be inferred from its shape, rendering the patterns which are both predictable and reproducible [10].

Within the realm of the bloodstain pattern classification, stains are categorized by their shape and distribution. They are separated into spatter stains and non-spatter stains based on their circular or non-circular formations. Spatter stains are further segregated into linear and non-linear categories, depending on the distribution of the bloodstains. While there are three distinct patterns within the linear spatter, there are four distinct patterns within the non-linear spatter. Linear bloodstains are characterized by a straightforward distribution, often appearing curvilinear, whereas non-linear bloodstains diverge in their distribution, spreading unpredictably across surfaces.

Turning to non-spatter stains, the classification depends on the regularity of the stain's borders. This leads to two primary patterns: those with irregular margins and those with regular ones. Within this category, a wide range of patterns emerges, including blood merging with other blood, such as heavy flows or splashes, smears, pattern transfers, saturation marks, and pooling. Lastly, there are certain patterns that do not fit the typical spatter and non-spatter classifications, meriting their unique miscellaneous category. This encompasses patterns like

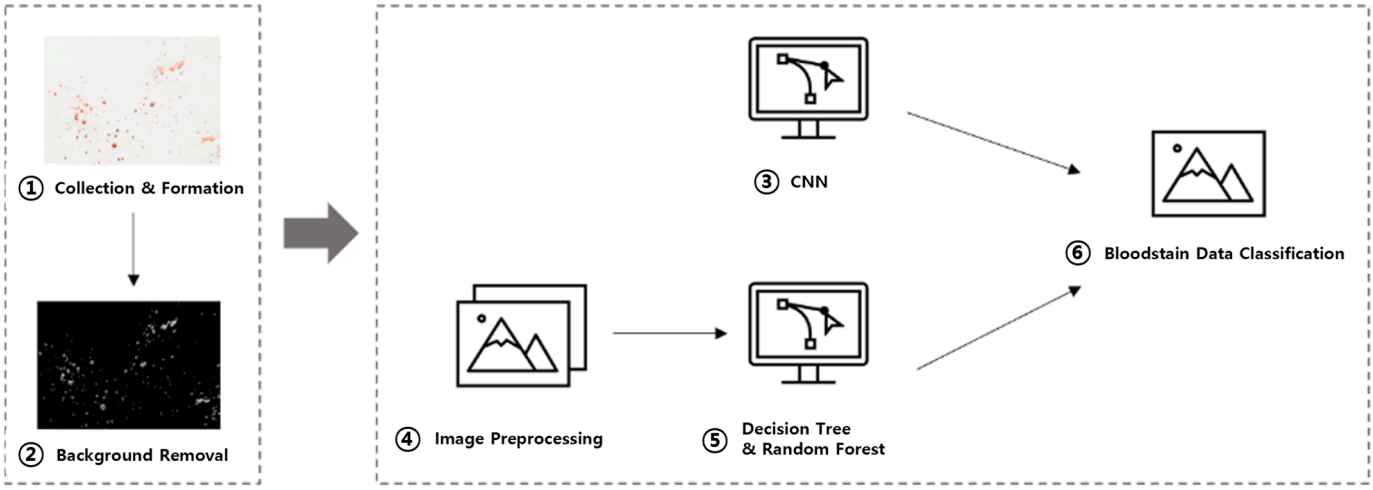

Fig. 1. Overall process of bloodstain type classification. The CNN model proceeds in the order of steps 1, 2, 3, and 6, while the decision tree model and random forest model follow the sequence of steps 1, 2, 4, 5, and 6.

capillary, skeletonized, void, and fly spots.

Prior research has depended on key reference points, such as an angle, the ratio of major axis to minor axis, and the shape of bloodstains, to methodically classify specific bloodstain images [11]. Once the background is eliminated and individual stains are isolated, the unique traits of each stain are meticulously assessed to determine its exact pattern classification.

2.2. Artificial intelligence technology

Classifying bloodstain patterns by eye takes a lot of work. While there are experts in bloodstain analysis, they are few in number. Consequently, the initiative to employ AI for classifying bloodstain images has gained considerable traction. The AI technology is used to automatically recognize and categorize visual patterns. Among a lot of AI methodologies, CNN [6] stands out; it directly assimilates patterns from image data, negating the necessity for manual feature extraction. This intrinsic capability of CNN has led to its widespread adoption in fields that demand object recognition like computer vision.

In the contemporary landscape, the integration of AI into bloodstain analysis is regarded as a marked rise. However, it is worth noting that the CNN model mandates an abundant amount of data to truly shine. This has encouraged research into ML models like a decision tree that extracts bloodstain features manually while leveraging AI capabilities [12]. In this paper, we are keen to explore a Random Forest model [8] and compare its effectiveness with that of a Decision Tree model [7].

3. Collection of bloodstain image data

In an effort to enhance the efficacy of AI models specifically tailored for BPA, a unique set of bloodstain shape image data was generated. The usage of human blood poses substantial biological hazards, and getting a large amount of it is complex. Similarly, animal blood, although it is an alternative, presents its own set of challenges including the potential for infections and sourcing difficulties. Given these constraints, this study opted to utilize "Spatter Blood" (produced by Sirchie, USA [13]), a synthetic blood substitute. This product is specifically designed for educational purposes related to BPA. Not only does it circumvent the inherent risks associated with human and animal blood, but it also closely copies the physical properties of human blood, including thickness, stickiness, and color.

In the process of generating bloodstain shape images for enhancing AI model training, the methodology described by Laber et al. served as a foundational reference [14]. To determine the most appropriate tools to simulate bloodstain formation, an exhaustive analysis was conducted on crime data provided by the National Police Agency, spanning 2011~2021. Out of an aggregate of 1,136,665 recorded arrests, 958,996 incidents were excluded due to the absence of any weapon or tool used in crime. From the residual 177,669 incidents, an in-depth examination revealed that knives were the predominant instrument of choice, implicated in 8,627 cases. The subsequent most recurrently employed tool was the hammer, evidenced in 7,131 cases [15]. The case number of each tool used in crime can be found in Table 1.

4. Bloodstain pattern data

In this section, we delve into the formation process of bloodstain pattern data and its subsequent preprocessing. For the purpose of this paper, we generated specific bloodstain pattern data for each type under examination. Unwanted backgrounds that were present during the capture of these bloodstain images were carefully removed in the preprocessing phase. Leveraging MATLAB [16], we precisely differentiate between these elements, as shown in Fig. 2. This delineation focuses on the contrasting luminosity between bloodstains and their surroundings. The employment of the methods that pinpoint these brightness disparities is crucial to emphasize the actual bloodstains while minimizing background distractions.

Table 1
The number of times of tools used in crime.

Criminal tool	Case
Knife	8627
Tool	7131
Computer	4078
Glass bottle	3355
Stone	1761
Cudgel	1397
Axe, sickle, farm equipment	489
String, tape, rope, wire	288
Poison	160
Mock firearms	86
Firearms	46
Anesthetic drugs	7
etc.	150,244
Total	177,669

Table 2
The number of times of bloodstain types found in crime.

Bloodstain	Formed	Provided	Total
Swing	23	61	84
Cessation	29	59	88
Impact	55	50	105
Total	107	170	277

4.1. Types of bloodstain pattern

Fig. 3 visually captures the tools employed for bloodstain production. A detailed classification of bloodstains is depicted in Fig. 4 [17]. This resulted in the formation of 84 Swing patterns, 88 Cessation patterns, and 105 Impact patterns. The number of data points used to create the image classification models is shown in Table 2. Unique characteristics are identified for each of these patterns, as described below:

- The *Swing* pattern is formed when an object coated with blood is swung, resulting in a linear distribution characterized by a progressive change in angle. This suggests that an object smeared with blood was used in a swinging motion at the crime scene. For experimental purposes, both a knife and a hammer were used to reproduce this specific pattern. The chosen instrument was dipped in blood and then swung from the top-right direction to the bottom-left, keeping a consistent 50 cm distance from the target surface intended for bloodstain capture.
- The *Cessation* pattern is observed when a blood-covered object is swung and abruptly halted, causing blood to disperse due to inertia. This pattern can either be linear or have an irregular shape, indicating that someone at the crime scene might have interrupted the motion of a bloodied object. In replicating this pattern, both a knife and a hammer were swung with the instrument initially immersed in blood. This swinging motion was performed at a steady 50 cm distance from the target surface. Once the motion ceased, the blood was allowed to form a distinct pattern on the designated surface.
- The *Impact* pattern emerges when a force is applied to a pool of blood, causing it to splatter away from its point of origin. This results in either a V-shaped or irregularly shaped stain. Such a pattern signifies that a dull object like a hammer was used to strike a pool of blood. In the experimental setup, layered wood was chosen as the base due to its firmness - a critical factor as a hard surface ensures effective blood dispersion upon forceful contact. The procedure entailed the dispensation exactly 1.4 ML of blood onto the plywood using a dropper, positioned 10 cm away from the designated bloodstain site. Following this, a sledgehammer was employed to strike the pooled blood, thereby creating the desired impact splatter.

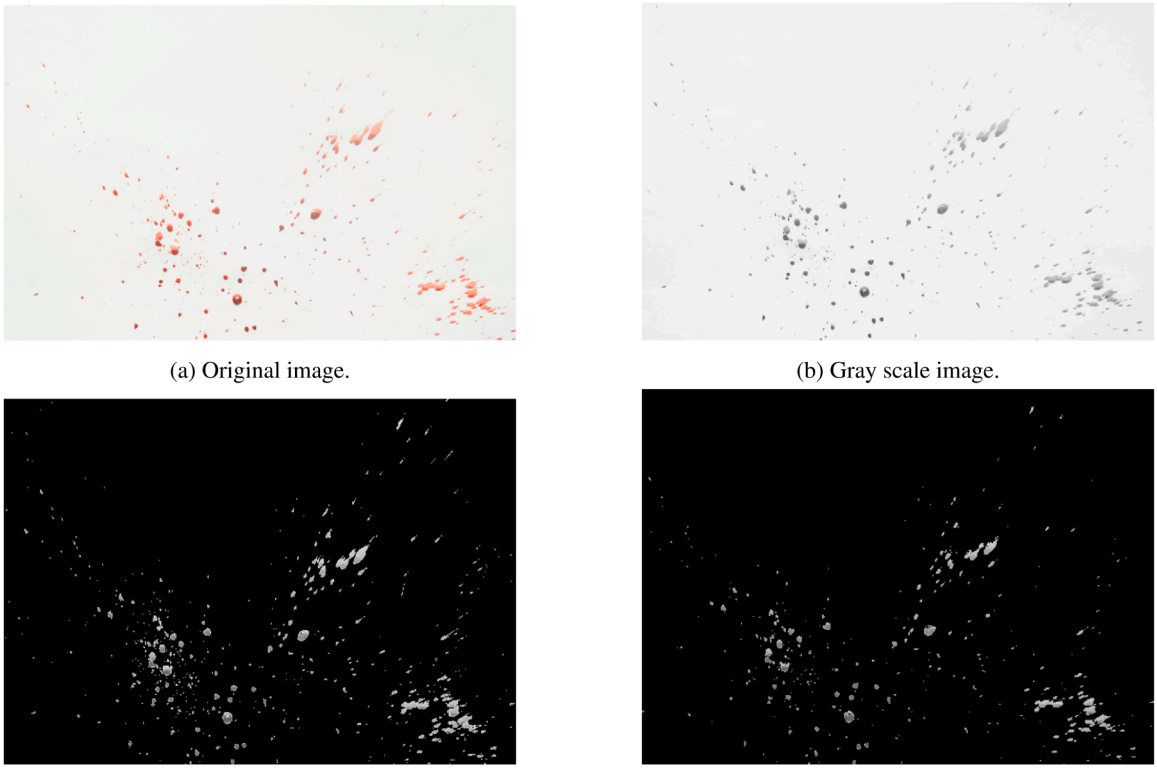

(a) Original image. (b) Gray scale image.

(c) Triangle method. (d) Ostu method.

Fig. 2. Process of extracting bloodstain data using MATLAB. (a) Original image. (b) Gray scale image. (c) Triangle method. (d) Ostu method.

Fig. 3. Bloodstain formation tools.

4.2. Data preprocessing

Bloodstain images typically display prominent bloodstain patterns against an extraneous background. Note that brightness values range from 0 (black) to 255 (white). For clarity in analysis, it is crucial to isolate these patterns from the background. This isolation helps eliminating the impact of the background. Fig. 2, which is created using the DIPImage of MATLAB Toolbox [18], illustrates the brightness distribution within the image.

In Fig. 2a, bloodstains blend with the background, making their brightness indistinguishable. In Fig. 2b, the image converted to grayscale to easily observe the bloodstain. Due to the brightness disparity, the bloodstains can be effectively isolated using the Triangle Method and Otsu's Method [9]. Figs. 2c and 2d show the results of these methods.

The Triangle Method draws a line from the histogram's peak to its end, determining the threshold based on the closest x-value. It excels in images with subtle contrast differences. In contrast, Otsu's Method uses histogram analysis to find an intensity level that separates the image into two categories by minimizing intraclass variance or maximizing between-class variance, making it ideal for bimodal histograms.

While the Triangle Method may preserve more noise, Otsu's Method is more effective at noise reduction. Given its superior capability in achieving clean background removal, Otsu's Method is preferred for data preprocessing.

There is a possibility that blood information can be lost when using these methods to remove the background. If the brightness of the background and bloodstain is similar, the bloodstain data can be removed when the background is removed. Also, if the size of the bloodstain is too small, the bloodstain data can be lost when the background is removed.

5. Bloodstain feature analysis in forensic context

Bloodstains serve as critical evidence in forensic context due to their distinct characteristics. This paper aims to separate these features into five specific groups by individual bloodstain distribution and an overarching distribution of the bloodstains.

5.1. Impact of angle feature extraction

The primary feature in this paper is the recurrent impact angle of the bloodstains. The Swing pattern is typified by a unidirectional impact angle, contrasting with the Impact pattern that encapsulates a myriad of angles. The angle of impact holds significant information to categorize the bloodstain. Fig. 5 delineates the color representation for the varied impact angles, divided into six sections:

- Blue: 0°–15°

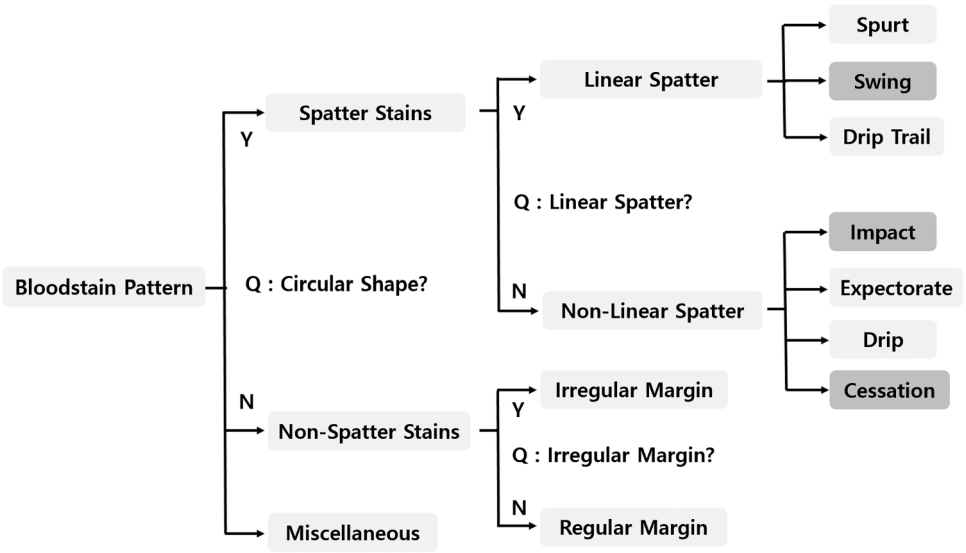

Fig. 4. Bloodstain classification system by appearance of bloodstain pattern. Analysis of swing, cessation, and impact in bloodstain patterns.

- Red: 15˚–30˚
- Green: 30˚–45˚
- Yellow: 45˚–60˚
- Pink: 60˚–75˚
- Cyan: 75˚–90˚

Notably, while the Impact pattern encompasses an array of angles, the Cessation pattern primarily exhibits one or two unique angles.

5.2. Irregularity analysis with bloodstain area and convex hull area

The subsequent feature subjected to examination is the shape of individual bloodstains. Most patterns evaluated in this paper showed a blend of circular and elliptical shapes. Due to their rapid trajectory, Swing and Impact patterns predominantly displayed elliptical bloodstains. In contrast, the Cessation pattern was primarily characterized by a circular form. To gain a more in-depth insight, the ellipticity ratio of a minimal ellipse emcompassing the convex for bloodstains was deduced using the ellipse's central point. Fig. 6 illustrates the classification based on stain appearance. Notably, irregular patterns with high ellipticity ratios are denoted in yellow (as ellipses) , while regular patterns with low ellipticity ratios are highlighted in green (as circles).

5.3. Circularity analysis for individual bloodstain

Our primary consideration in this analysis was the ratio of the major axis to the minor axis of individual bloodstains. Whenever a bloodstain exhibited a tail, it was meticulously removed using MATLAB to ensure accurate evaluation of the axis ratios. As illustrated in Fig. 7, this process emphasizes the inherent shape of the tail-free bloodstain. Notably, circular bloodstains are highlighted in blue while the elliptical ones are in pink. Our assessment relied exclusively on these tail-free bloodstains to ascertain the axis ratios. An increase in this ratio typically indicated an elliptical shape. By examining the relationship between the lengths of the major and minor axes, we were able to distinguish between the circular and elliptical forms of bloodstains.

The definition of a bloodstain's circularity can be expressed by the following equation:

$$\text{Circularity} = \frac{\text{Length of the major axis} - \text{Length of the minor axis}}{\text{Length of the major axis}}. \quad (1)$$

We set a definitive threshold value:

$$\text{Threshold} = 0.3 \quad (2)$$

The classification based on this threshold is:

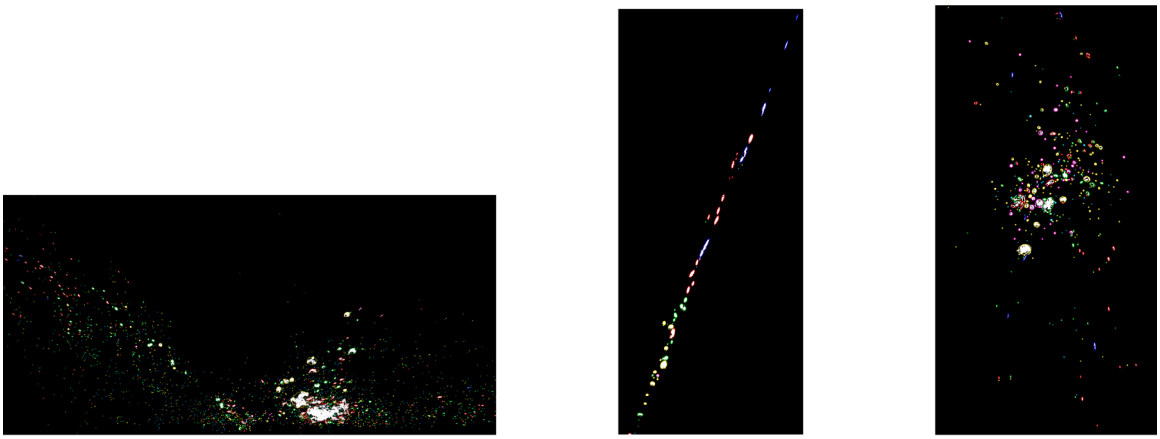

(a) Impact. (b) Swing. (c) Cessation.

Fig. 5. The impact angle feature extraction.

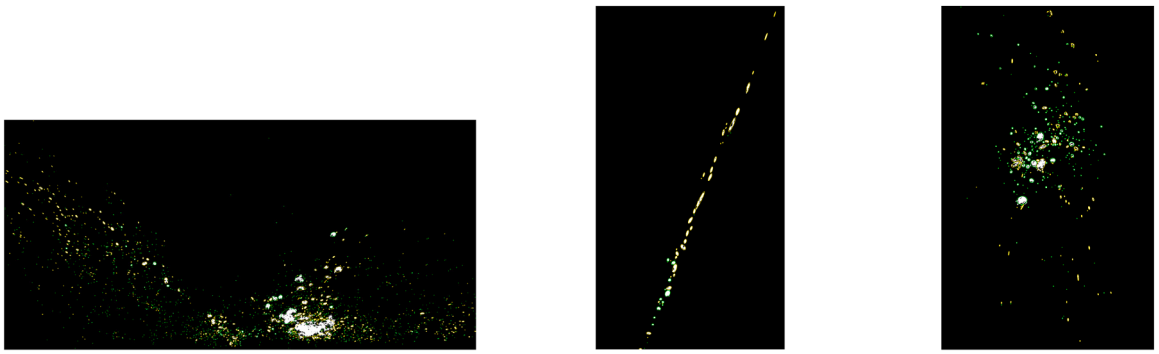

(a) Impact. (b) Swing. (c) Cessation.

Fig. 6. The irregularity analysis using a ratio of each bloodstain area to convex hull area.

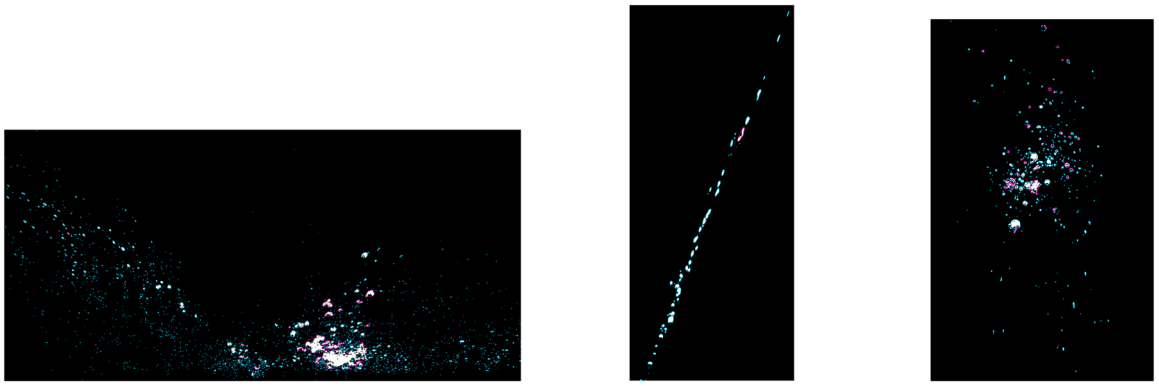

(a) Impact. (b) Swing. (c) Cessation.

Fig. 7. The circularity analysis for individual bloodstain.

$$\text{Circular bloodstain if Circularity} < \text{Threshold}, \tag{3}$$

$$\text{Elliptical bloodstain if Circularity} > \text{Threshold}. \tag{4}$$

5.4. Convex hull of whole individual bloodstains

The fourth analytical feature depended on the overall spatial distribution formed by the convex hull which is the tightest boundary encapsulating all individual bloodstains (shortly called stains). As the distribution of bloodstains broadens, the convex hull's area is amplified accordingly. Empirical observations highlighted the maximum stain distribution in the Impact pattern, with the minimum being observed in the Swing pattern. Fig. 8 depicts the spatial extent of the convex hull with respect to each stain.

5.5. Linearity analysis with polynomial regression equation

Finally, the comprehensive distribution of bloodstains was assessed using a linear regression approach [11]. By determining the centroid for each stain, a regression line was ascertained, minimizing the aggregate error distance between the line and individual stains. Fig. 9 displays the linear regression analysis derived from bloodstain centroids.

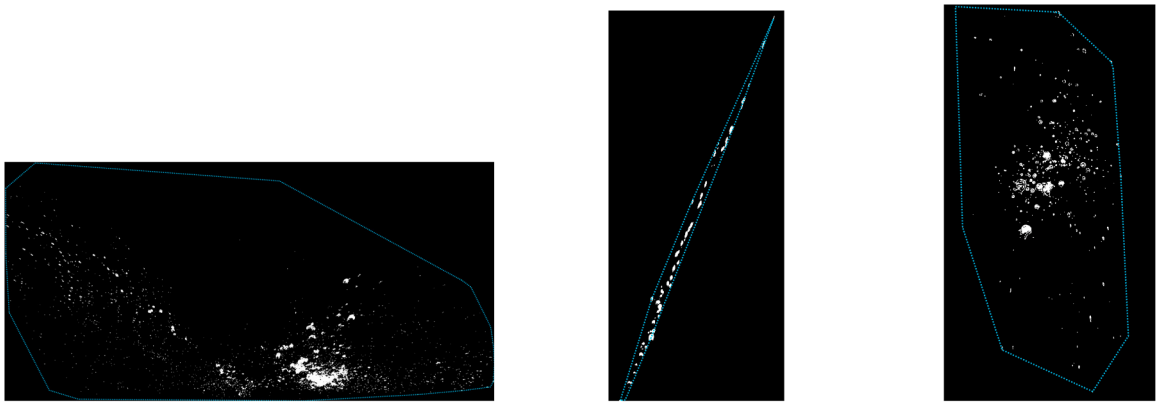

(a) Impact. (b) Swing. (c) Cessation.

Fig. 8. The convex hull of whole individual bloodstain.

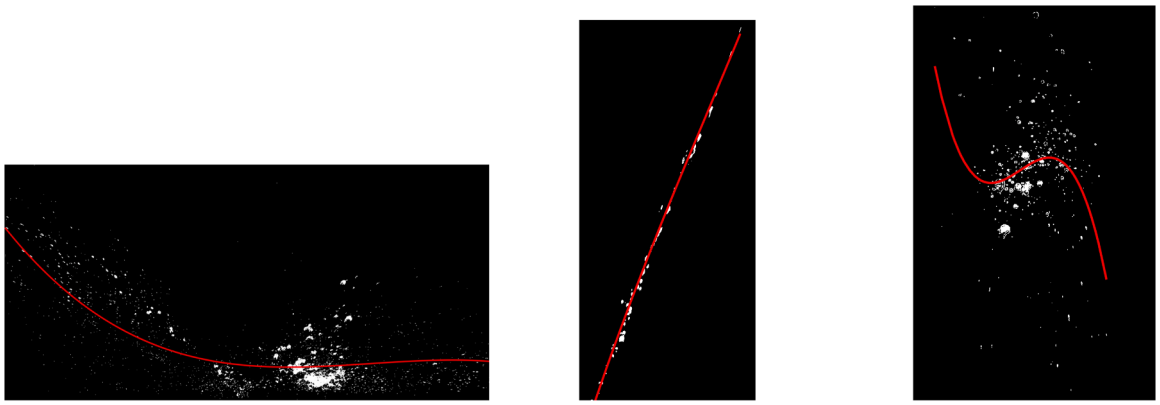

(a) Impact. (b) Swing. (c) Cessation.

Fig. 9. The linearity analysis using polynomial regression equation.

This regression line assists in determining the trajectory with the minimal aggregate distance error. Thus, a limited spread corresponds to the Swing pattern, while a larger variance typifies the Impact pattern. The Cessation pattern showing a radial distribution poses challenges for bloodstain type prediction using linear regression.

Subsequently, we extracted a feature representing the average sum of distances between all individual bloodstains in an image data and a tertiary function. The Euclidean distance d used for two points (x_i, y_i) and (x_j, y_j) is defined by:

$$d = \sqrt{(x_i - x_j)^2 + (y_i - y_j)^2}. \quad (5)$$

6. Design and implementation of ML models

This section explains the CNN, Decision Tree, and Random Forest models for bloodstain pattern analysis. We utilize datasets comprising 84 Swing patterns, 88 Cessation patterns, and 105 Impact patterns.

6.1. Convolutional Neural Network (CNN)

The CNN is a multilayered feed-forward artificial neural network, specifically crafted for visual image analysis [6]. It integrates filtering methods into an artificial neural network and classifies images by learning adaptively data using filter matrices. This deep learning technique promotes efficient image processing. During the training phase, the test dataset was prepared by subtracting 20 % from the dataset. From the remaining 80 % of the dataset, 65 % and 15 % were used as the training dataset and the validation dataset, respectively. We employed the Image Data Generator with a setting including rescale = 1.255, rotation range = 10, width shift range = 0.1, height shift range = 0.1, shear range = 0.1, and zoom range = 0.8.

6.2. Decision tree

A key of a decision tree model is its classification criteria [7]. The decision tree represents decision rules in a tree structure, where internal nodes span from the root node to the terminal nodes. Employing a tree of maximal depth on novel data may induce overfitting, hindering generalization. To mitigate this, we incorporated pruning techniques. Parameters such as maximum depth, maximum leaf nodes, minimum leaf nodes, and minimum data per node were adjusted to prevent excessive branching. For our experiments, x-value encompassed classified features, while y-value pertained to the target labels. Data was divided into training and test sets in an 8:2 ratio, with the tree's maximum depth limited at 10.

6.3. Random forest

The Random Forest model [8] addresses the inherent limitations of the decision tree, especially its sensitivity to training data and a sequence of decision criteria in a tree. Random forest integrates multiple decision trees and the outcome is based on a majority vote. Each tree is constructed using bootstrap sampled datasets. Bagging and boosting as ensemble techniques in pattern recognition are pivotal in constructing a random forest. In our experiments, y-value stored the correct labels, and x-value contained the features. Data was devided into training and test sets in an 8:2 ratio. To optimize accuracy, we set the number of estimators (called n_estimators) at 98, with the maximum tree depth limited to 4. We chose the number of estimators as 98 because the accuracy did not improve beyond 98.

6.4. Bloodstain type classification process

Fig. 1 illustrates the process of bloodstain type classification with data processing steps. The first step entails data collection and generation. Following the data collection, background subtraction is performed to improve bloodstain data extraction. Subsequently, the image is fed into the CNN model. On the other hand for decision trees and random forests, features are manually extracted from the data, and the data values are input into each model. In the classification model, bloodstain patterns are identified and categorized by types. The model's accuracy is assessed by comparing predicted values with actual values.

7. Performance evaluation

This section investigates the performance accuracy of the three different models implemented in this paper. Notably, the Random Forest classifier outperformed other two models, showing an accuracy of approximately 80 %.

7.1. Evaluation of CNN

Figs. 10 and 11 provide a graphical representation of the training outcomes of the CNN model. While the accuracy graph in Fig. 10 showed a trend of improvement, the loss graph in Fig. 11 demonstrated a decrease over iterations. With test data, the overall accuracy of the CNN model stood at approximately 52 %. We can also recognize the influence of the features shown in Fig. 12 which are used as input to the CNN model in order to identify the bloodstain patterns. We can see that Angle_var (i.e., Angle Variance) has the highest influence on identifying the bloodstain patterns.

When evaluated on 54 test data samples, shown in Fig. 13a, our CNN model achieved an accuracy of 51.9 %, correctly classifying 28

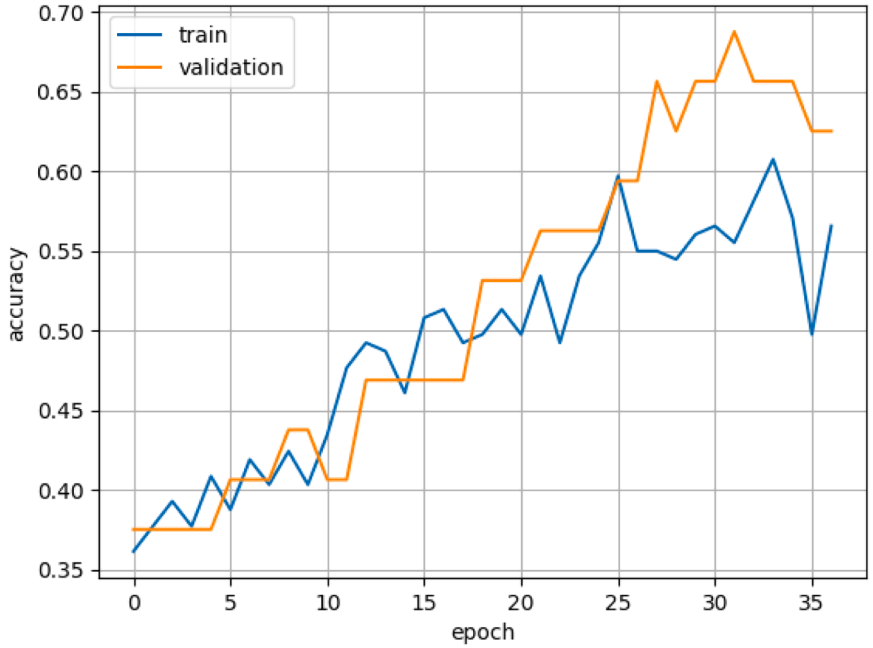

Fig. 10. Accuracy of CNN. Accuracy gradually increases.

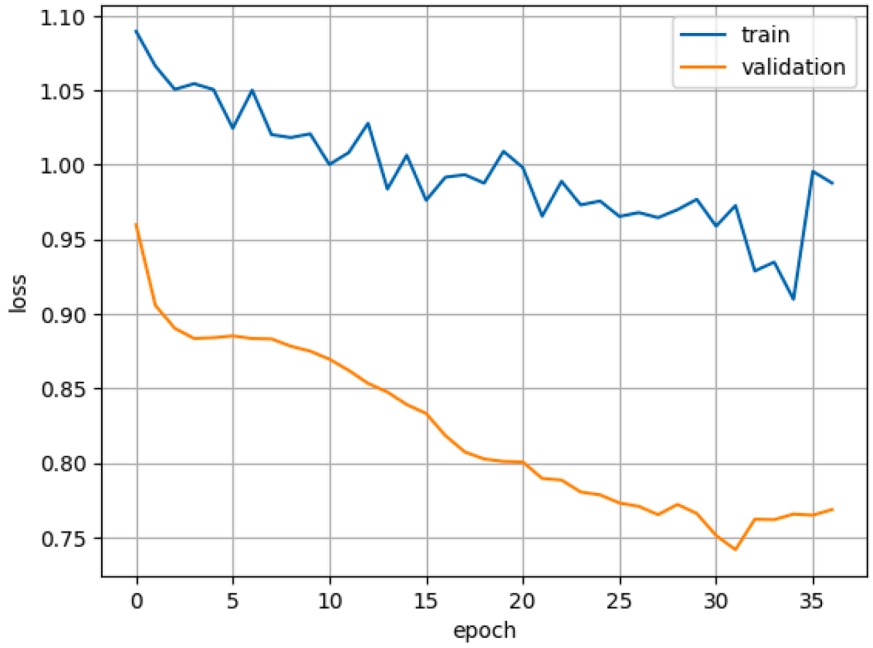

Fig. 11. Loss of CNN. Loss gradually decreases.

instances. However, 26 samples were misclassified, leading to an error rate of 48.1 %. This suggests potential avenues for further refining the model. One reason for this is the feature similarity (shown in Fig. 12) between Swing and Cessation patterns while the primary difference is the overall shape of the bloodstain distribution: Swing has a linear shape and Cessation has a non-linear shape. The CNN model's limited accuracy may arise from not effectively distinguishing between these nuances.

7.2. Evaluation of decision tree

The Decision Tree model achieved an accuracy of around 72 %. The optimal results were obtained with the tree's maximum depth set at 10. This particular depth was chosen because increasing it beyond 10 does not lead to an improvement in accuracy. In other words, the accuracy is not improved for depths greater than 10. The confusion matrix, shown in Fig. 13b, was drawn from 56 test data points. Out of these, 40 were in alignment with the model's predictions, whereas 16 were not.

7.3. Evaluation of random forest

The Random Forest classifier emerged as the most efficient model with an accuracy of approximately 80 %, surpassing both the CNN and Decision Tree models. Among the features, the linear feature was considered most critical, with the rest holding roughly equal significance. The confusion matrix for this model, depicted in Fig. 13c, was based on 56 test data points. Among these instances, the model's

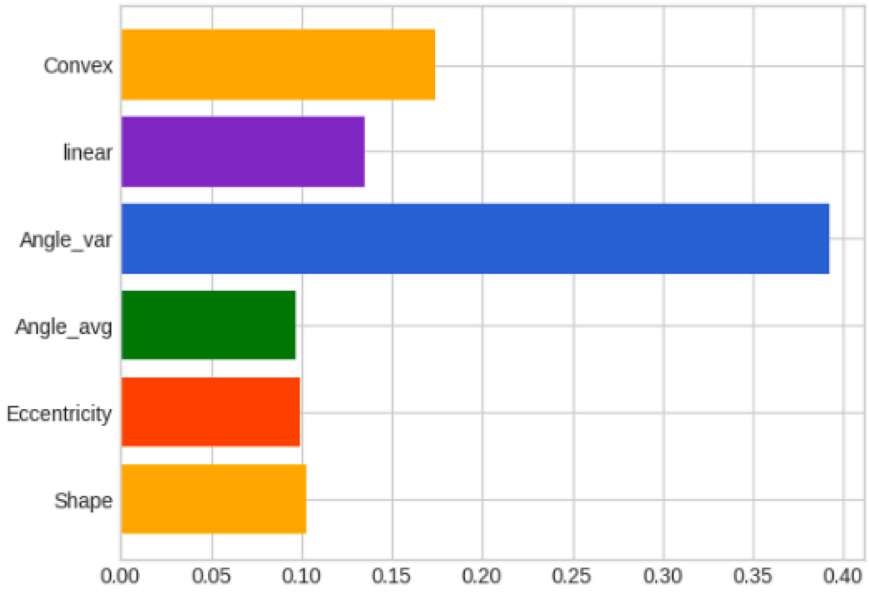

Fig. 12. Feature importance.

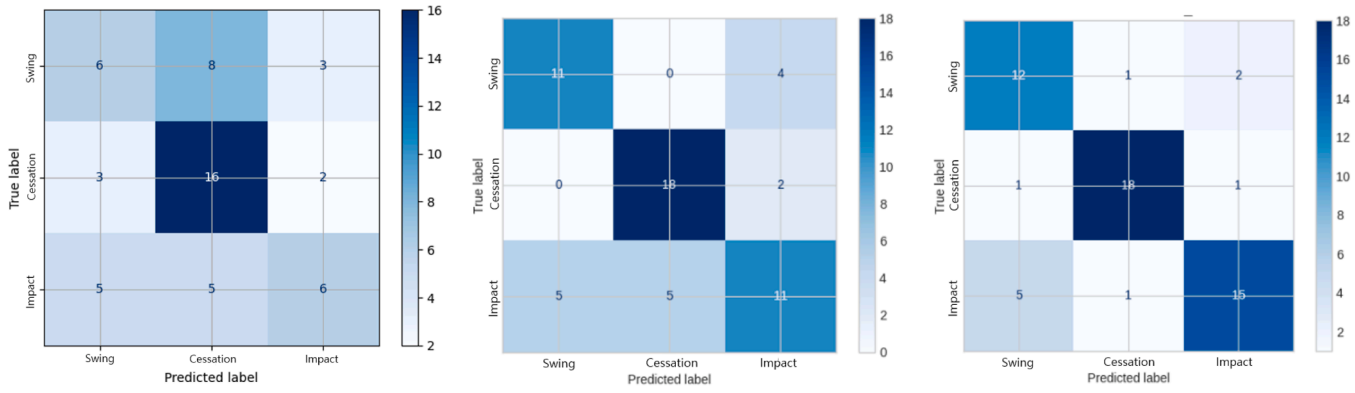

(a) CNN. (b) Decision tree. (c) Random forest.

Fig. 13. Confusion matrix.

predictions matched 45 instances, while 11 instances deviated from the expected outcomes. The CNN had a lower accuracy because it was trained on a small-sized dataset of bloodstain images, whereas the Decision Tree and Random Forest models were trained well even with bloodstain features from a small-sized dataset of bloodstain images. Random Forest works better than Decision Trees because it uses many trees to make predictions, which helps to avoid mistakes. It looks at different features for each tree, leading to more accurate results. It is also strong against errors and can show which features are most important.

8. Conclusion

This paper proposes a machine learning-based framework for an automatic bloodstain classification at a crime scene for forensic science. For the bloodstain patterns observed in this paper, we employed spatter blood, an artificial blood substitute from Sirchie company (USA) designed for training purposes. While this substitute does have a few differences compared to human blood, future research could utilize human blood or animal blood such as porcine, bovine, or sheep. In this paper, experiments were conducted based on limited distance and limited amount of blood while generating bloodstain patterns using Spatter Blood in the laboratory. Therefore, the bloodstains shown in the paper only implemented 20 % of the bloodstains that can be created, and the experiment was conducted by selecting the patterns that are generally most difficult to distinguish among them. We focused on classifying three challenging types of bloodstain patterns which are difficult to distinguish from one another: Swing, Cessation, and Impact. This is because in actual crime scenes, the most easily confused bloodstain patterns are Swing, Cessation, and Impact. The latter Expectorate patterns, which are categorized as non-linear spatter patterns, are created when individuals cough up blood. Given the potential biological dangers and health risks of using real human blood, especially simulating expectoration by holding the blood in one's mouth, future studies could incorporate safe human blood or design tools that can replicate a cough's pressure for generating Expectorate patterns.

Bloodstain pattern classification, an integral part of Bloodstain Pattern Analysis (BPA), was executed in this paper using AI. Bloodstains can offer invaluable insights at crime scenes, aiding in the reconstruction of events by analyzing the patterns they form. Through our research, we employed AI, using a Convolutional Neural Network (CNN), decision tree, and random forest models, to classify these patterns. Among the models, the random forest demonstrated superior performance where the accuracies of those three models (i.e., CNN, decision tree, and random forest) were 52 %, 72 %, and 80 %, respectively. However, there are limitations to using the CNN model. This model has the disadvantage of not being able to classify bloodstains well

if the size of the bloodstain is too small. Also, if the background brightness is too bright, it is difficult to separate the bloodstains from the background. Therefore, to use these three models, the classification framework must first check whether the size of the bloodstain and the brightness of the background are adequate or not.

As future work, to elevate the accuracy of our models, we will consider other methods: augmenting the dataset, introducing new features to differentiate the bloodstain types, and experimenting with other model architectures like support vector machines and naive Bayes methods.

CRediT authorship contribution statement

Jaehoon (Paul) Jeong: Writing – review & editing, Validation, Supervision, Resources, Methodology, Investigation, Funding acquisition, Conceptualization. **Si-Keun Lim:** Writing – review & editing, Supervision, Project administration, Investigation, Funding acquisition, Conceptualization. **Yoseop (Joseph) Ahn:** Writing – original draft, Visualization, Validation, Software, Methodology, Investigation, Formal analysis, Data curation, Conceptualization. **Hyeonah Jung:** Writing – original draft, Visualization, Validation, Methodology, Investigation, Formal analysis, Data curation, Conceptualization. **Yeon-Soo Jo:** Writing – original draft, Resources, Methodology, Formal analysis, Data curation.

Declaration of Competing Interest

The authors declare the following financial interests/personal relationships which may be considered as potential competing interests: The corresponding author reports financial support was provided by his government. If there are other authors, they declare that they have no known competing financial interests or personal relationships that could have appeared to influence the work reported in this paper.

Acknowledgements

This work was supported by the National Research Foundation of Korea (NRF) grant funded by the Korea government, Ministry of Science and ICT (MSIT) (No. 2023R1A2C2002990). This work was supported in part by the Institute of Information & Communications Technology Planning & Evaluation (IITP) grant funded by the Korea government, Ministry of Science and ICT (MSIT) (No. RS-2022-II221199, Regional strategic industry convergence security core talent training business). This work was supported in part by AI Convergence Research Fund, Sungkyunkwan University, 2022. Some of data used for modeling were provided by National Forensic Service, Gangwon Provincial Police, and S. Y. Lee.

References

[1] O. Peschel, S. Kunz, M. Rothschild, E. Mützel, Blood stain pattern analysis, Forensic Sci., Med., Pathol. 7 (2011) 257–270.
[2] H.C. Lee, C. Ladd, Preservation and collection of biological evidence, Croat. Med. J. 42 (3) (2001) 225–228.
[3] E. Mistek, M.A. Fikiet, S.R. Khandasammy, I.K. Lednev, Toward locard's exchange principle: recent developments in forensic trace evidence analysis, Anal. Chem. 91 (1) (2018) 637–654.
[4] H.C. Lee, E.M. Pagliaro, Forensic evidence and crime scene investigation, J. Forensic Investig. 1 (2) (2013) 1–5.
[5] T. Bevel, R.M. Gardner, Bloodstain pattern analysis with an introduction to crime scene reconstruction, CRC Press, 2008.
[6] P. Kim, Convolutional neural network, MATLAB deep learning: With Machine Learning, Neural Networks and Artificial Intelligence (2017) 121–147.
[7] Y.-Y. Song, L. Ying, Decision tree methods: applications for classification and prediction, Shanghai Arch. Psychiatry 27 (2) (2015) 130.
[8] A. Liaw, M. Wiener, et al., Classification and regression by randomforest, R. N. 2 (3) (2002) 18–22.
[9] N. Otsu, A threshold selection method from gray-level histograms, IEEE Trans. Syst., Man, Cybern. 9 (1) (1979) 62–66.
[10] C. Knock, M. Davison, Predicting the position of the source of blood stains for angled impacts, J. Forensic Sci. 52 (5) (2007) 1044–1049.
[11] R.M. Arthur, P.J. Humburg, J. Hoogenboom, M. Baiker, M.C. Taylor, K.G. de Bruin, An image-processing methodology for extracting bloodstain pattern features, Forensic Sci. Int. 277 (2017) 122–132.
[12] R. Arthur, J. Hoogenboom, M. Baiker, M. Taylor, K. De Bruin, An automated approach to the classification of impact spatter and cast-off bloodstain patterns, Forensic Sci. Int. 289 (2018) 310–319.
[13] D. Attinger, C. Moore, A. Donaldson, A. Jafari, H.A. Stone, Fluid dynamics topics in bloodstain pattern analysis: comparative review and research opportunities, Forensic Sci Int. 231 (1-3) (2013) 375–396. Sep 10.
[14] T. Laber, P. Kish, M. Taylor, G. Owens, N. Osborne, J. Curran, Reliability assessment of current methods in bloodstain pattern analysis, Final Report for the National Institute of Justice. US In: National Institute of Justice (2014).
[15] N.P. Agency, National police agency crime statistics (2023).
[16] S. Matlab, Matlab, The MathWorks, Natick, MA (2012).
[17] G.P.P. Agency, Bloodstain morphology analysis guidebook (2019).
[18] C.L.L. Hendriks, DIPimage: A Scientific Image Processing Toolbox for MATLAB (2005).